

# Holographic magnetic imaging of single layer nano-contact spin transfer oscillators.

Erick O. Burgos Parra<sup>1</sup>, Nick Bukin<sup>1</sup>, Maxime Dupraz<sup>2</sup>, Guillaume Beutier<sup>2</sup>, Sohrab Redjai Sani<sup>3</sup>, Horia Popescu<sup>4</sup>, Stuart A. Cavill<sup>5</sup>, Johan Åkerman<sup>6,3</sup>, Nicolas Jaouen<sup>4</sup>, Paul S. Keatley<sup>1</sup>, Robert J. Hicken<sup>1</sup>, Gerrit van der Laan<sup>7</sup> and Feodor Y. Ogrin<sup>1</sup>

<sup>1</sup>Department of Physics and Astronomy, University of Exeter, Exeter, Devon, UK.

<sup>2</sup>SIMaP, Grenoble-INP, CNRS, Grenoble, France.

<sup>3</sup>Material Physics, KTH- Royal Institute of Technology, Kista, Sweden.

<sup>4</sup>SOLEIL synchrotron, Paris, France.

<sup>5</sup>Department of Physics, University of York, York, North Yorkshire, UK.

<sup>6</sup>The Physics Department, University of Gothenburg, Gothenburg, Västra Götaland, Sweden.

<sup>7</sup>Diamond Light Source Ltd., Didcot, Oxfordshire, UK.

**Time-averaged images of the magnetization within single layer spin transfer oscillators have been obtained using the holography with extended reference by autocorrelation linear differential operator (HERALDO) technique. Transport measurements on a Pd(5)-Cu(20)-Ni<sub>81</sub>Fe<sub>19</sub>(7)-Cu(2)-Pd(2) (in nm) stack with a 100 nm diameter nano-contact reveal the presence of vortex dynamics. Magnetic images of the device for injected current values of 24mA and -24mA suggest that a vortex has been ejected from the nano-contact and become pinned at the edge of the region that is visible through the Au mask.**

*Index Terms*—HERALDO, Magnetic vortex, Spin transfer torque, X-ray holography.

## I. INTRODUCTION

THE DISCOVERY of Spin Transfer Torque (STT) [1] has led to a range of new dynamic magnetic effects and devices that are not only fundamentally interesting but also have direct applications in the areas of microwave technology and communications. In one such device, the nano-contact spin-torque oscillator (NC-STO), the STT excites precession of the magnetization and perfectly balances the damping, leading to the appearance of auto-oscillations [2, 3]. This effect is of great interest for microwave technology, as it paves the way for a new class of tunable microscopic microwave generators. While the majority of NC-STO devices exploit giant magneto-resistance (GMR) trilayer systems, in order to achieve large STT, a number of similar effects were demonstrated in devices based upon single ferromagnetic layers [4, 5, 8, 9]. Theory predicts [10, 11] that a spin torque, of similar strength to that obtained with GMR materials, can be achieved via asymmetric spin-accumulation at the different interfaces of a single layer ferromagnetic pillar [6, 7]. In a recent experimental study [12], it was suggested that NC-STO devices can also be realized on extended single-layer ferromagnetic films. Experiments carried out on a Pd<sub>5</sub>-Cu<sub>20</sub>-NiFe<sub>7</sub>-Cu<sub>2</sub>-Pd<sub>2</sub> (thicknesses in nm) stack, showed that a microwave signal can be generated with power and line width values comparable to those achieved with GMR materials. Moreover the microwave emission did not require application of an external magnetic field, making it much more favourable for technological applications.

Although the observed effect is obviously related to the magnetization dynamics in the NiFe magnetic free layer, the

exact nature of the dynamics is not well understood. Given the range of the generated microwave frequencies, which may be as low as 250 MHz, it has been suggested that the emitted signal must originate from the gyrotropic motion of vortices, which have been commonly observed for equivalent NC-STO devices based on GMR materials. However, the observation of microwave emission at frequencies up to 3 GHz appears incompatible with the gyration of a single vortex. Instead this behavior was ascribed to the repeated creation and annihilation of a vortex-antivortex (V-AV) pair underneath the nano-contact [13]. Moreover, it was proposed that the process could involve two V-AV pairs with opposite polarizations [14].

In this paper we investigate the magnetization dynamics of a single layer NC-STO by means of the recently developed soft x-ray imaging technique known as holography with extended reference by autocorrelation linear differential operator (HERALDO) [15, 16]. This technique can provide high spatial resolution (~20 nm) with immunity to mechanical and thermal drifts. A particular advantage of HERALDO compared to the standard Fourier Transform Holography (FTH), is its ability to image both ‘out-of-plane’ and ‘in-plane’ components of the magnetization. This is of direct relevance to systems containing magnetic vortices where both in and out of plane magnetization components are present.

## II. EXPERIMENTAL PROCEDURE

### A. Sample

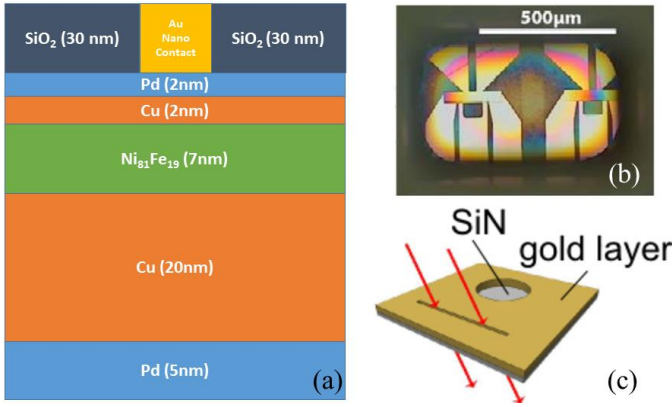


Fig. 1. Schematics of a single layer NC-STO, (a) layer composition, (b) coplanar waveguide (CPW) with the NC-STO fabricated on a  $\text{Si}_3\text{N}_4$  membrane for imaging at 45 degrees incidence by HERALDO, (c) Reference slit and gold mask orientation in case of off-normal orientation with the beam.

A non-magnetic/ferromagnetic/non-magnetic stack of composition Pd(5)-Cu(20)-Ni<sub>81</sub>Fe<sub>19</sub>(7)-Cu(2)-Pd(2) (thicknesses in nm) was built on top of a  $\text{Si}_3\text{N}_4$  membrane using the procedure described in reference [12]. The lithographically integrated nano contact (NC) used to drive current through the device had 100nm diameter. Figure 1 shows a schematic of the device and the co-planar waveguide (CPW) used to supply the current. To obtain a holographic image, the sample has a slit of 35nm width and 6 $\mu\text{m}$  length that is separated from the imaged area by a distance of 11  $\mu\text{m}$ , which is within the x-ray coherence length.

### B. Electrical measurements

Transport measurements were performed by supplying a DC current to the sample through the DC port of a bias-tee, while the microwave signal generated by the STT effect was measured simultaneously through the AC port. The microwave signal was input to a preamplifier and then a spectrum analyzer.

### C. HERALDO

In order to image the magnetization dynamics of the sample, soft x-ray holography was performed using the HERALDO technique that was previously used to image static magnetic vortices [13,15]. Measurements were made at the SEXTANTS beamline at the SOLEIL Synchrotron (Paris, France) in order to obtain a highly coherent x-ray beam. Samples grown on  $\text{Si}_3\text{N}_4$  membranes allow transmitted x-rays to pass to a CCD camera, positioned on the optical axis behind a beam-stop that removes the direct beam as is shown in Fig. 2(a). The interference pattern of the beam transmitted by the sample and the reference slit are recorded on the CCD camera as is shown in Fig. 2(b). By taking directional derivatives of the Fourier transform of the raw image (Fig. 2(c)), the real space image may then be recovered [7].

## III. RESULTS AND ANALYSIS

Fig. 3 shows the characteristic voltage spectral density of the -microwave signal generated by a single layer NC-STO with

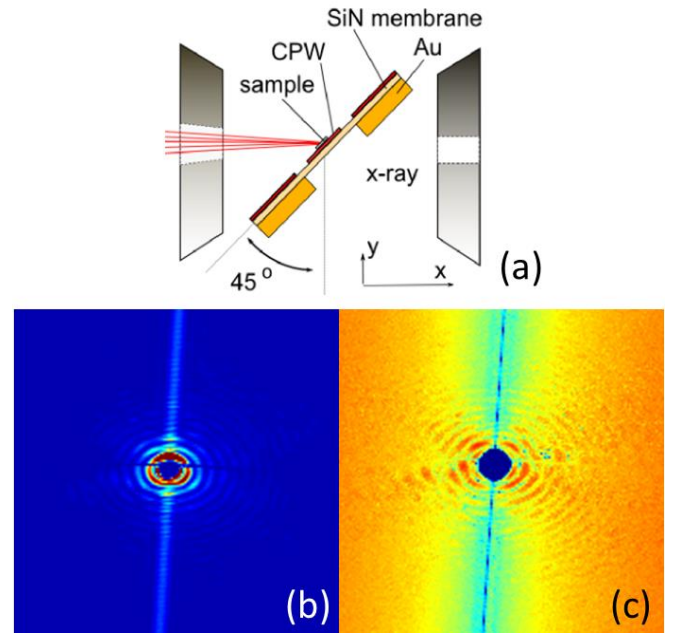


Fig. 2. (a) Orientation of the sample with respect to the x-ray beam. (b) Log-scale diffraction pattern captured by the CCD camera for one x-ray polarization. The slanted vertical line is produced by the reference slit and the dark blue circle in the center and the blue line passing through the image are from the beamstop and its holder respectively. (c) Diffraction pattern after normalization, removal of the central beamstop region and with the differential filter applied. The inverse Fourier transform of this image then yields the real and imaginary parts of real space charge (structure) and magnetism distribution.

110 nm contact diameter when the current is swept from -30 mA to 0 mA. Up to 3 harmonics of the fundamental frequency signal are observed, as well as mode transitions at  $\sim -20$  mA,  $-15$  mA and  $-7$  mA. The linewidth decreases substantially from  $\sim 36$  MHz to 10 MHz as the current is decreased from  $-23.5$  mA to  $-12.5$  mA, while the microwave frequency exhibits a quasi-linear dependence on current for values between  $-15$  mA and  $-7$  mA. All the observed features of the signal, including a hysteretic dependence of the frequency upon current, a continuous monotonic dependence of frequency upon current,

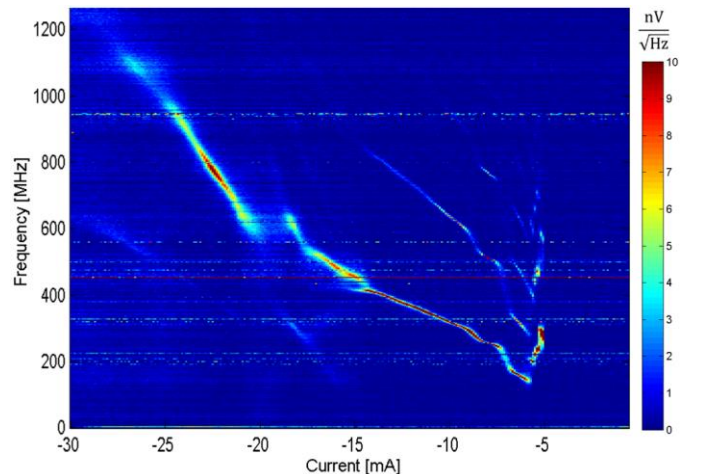


Fig. 3. Dependence of the microwave frequency on DC current for a SL STO with 110 nm nano-contact diameter. The current was varied from -30 mA to 0 mA at zero applied magnetic field.

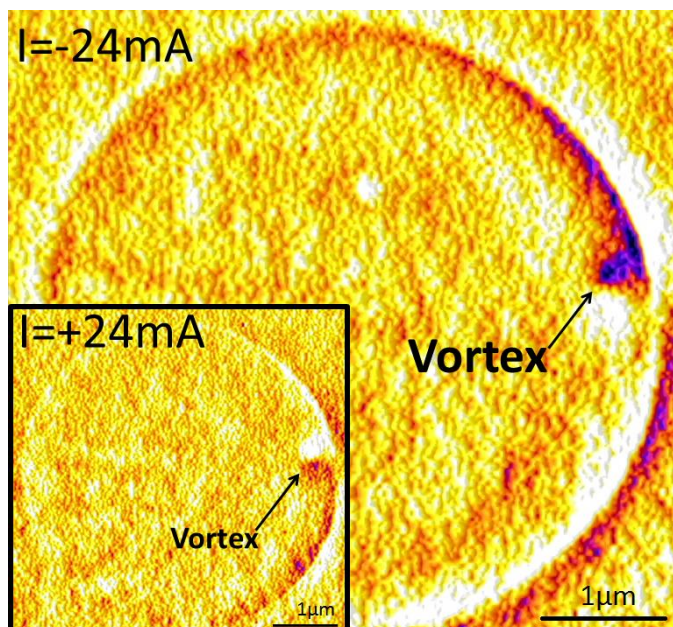


Fig. 4 HERALDO reconstruction of difference interference patterns obtained by subtracting interference patterns obtained with right and left circular polarization. The images were acquired from a SL-STO device at current values of  $-24\text{mA}$  and  $24\text{mA}$ . Blue and white denote in-plane magnetization components pointing to the right and left respectively. Measurements were taken with x-rays at  $45^\circ$  grazing angle and with energy of  $706.5\text{ eV}$

and a broad range of emission frequencies ( $150\text{ MHz} - 2\text{GHz}$ ) are consistent with the suggested mechanism of V-AV creation and annihilation under the NC induced by the Oersted field [6]. For current values less than that required for nucleation, the V-AV creation and annihilation is expected to stop, with the generated microwave power increasing due to the continuous motion of a single vortex.

In order to observe the vortex dynamics in the sample, images were acquired, using the HERALDO technique, from devices with  $100\text{nm}$  and  $50\text{nm}$  contact diameter. The magnetic state was imaged for different values of the DC current with x-rays of  $706.5\text{ eV}$  energy incident at  $45$  degrees to the sample normal, with the plane of the incidence lying in the horizontal direction within the image. The energy used correspond to the L3 Fe edge and was used in order to obtain the magnetic information from the NiFe layer. Fig. 4 shows the holograms reconstructed from difference interference patterns acquired at current values of  $-24\text{mA}$  and  $24\text{mA}$ . The difference interference patterns are obtained by subtracting interference patterns acquired with positive and negative circular x-ray polarization, each of which is the average of  $\sim 800$  exposures of  $60\text{ms}$  duration. Both current polarities show magnetic contrast suggestive of vortex formation just within the edge of the aperture within the gold layer. The polarity of the contrast, and hence the orientation of the magnetization within the vortex, are seen to reverse with the polarity of the current as might be expected. As well as the *vortex*-like feature, contrast reminiscent of a domain wall is observed along the rim of the aperture. The measurements without the DC current showed no contrast. Measurements at lower currents showed similar effects though with reduced contrast.

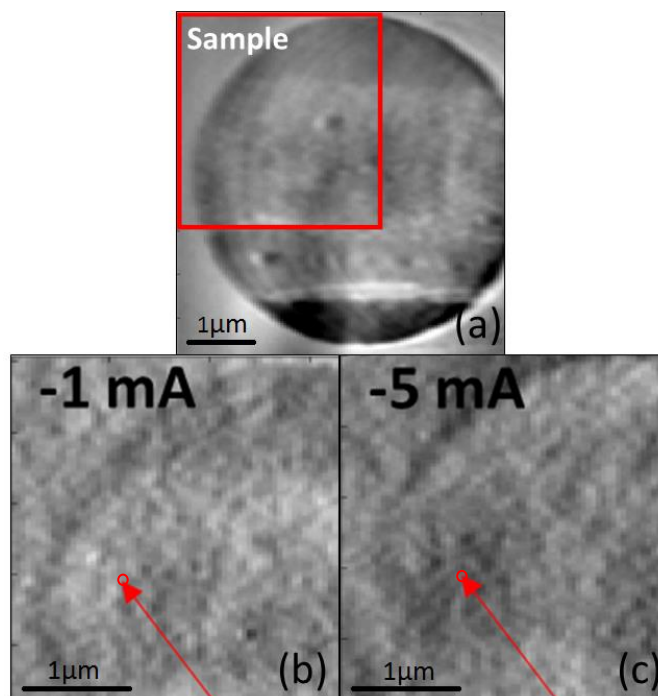


Fig. 5. HERALDO reconstructions for a SL-STO device. (a) Aperture in the gold mask providing access to the underside of the stack (non-magnetic image). The red square encloses the region of the sample for which magnetic contrast is shown in (b) and (c). (b), (c) Magnetic images of a SL-STO device at  $-1\text{mA}$ , and  $-5\text{mA}$  respectively. The red arrow shows where the NC (red circle) is positioned.

An analysis based upon preliminary micromagnetic simulations (not shown here) leads to the following interpretation. The vortex structure is observed some way from the NC, which is positioned near the middle of the aperture. It is therefore expected that a V-AV structure is initially formed underneath the NC, before the vortex is ejected due to the large gradient in the confining potential associated with this relatively large current value. The vortex then becomes pinned at the rim of the aperture. It is likely that the magnetic layer is highly stressed at the rim due to the physical removal of the gold layer behind the  $\text{Si}_3\text{N}_4$  membrane. The mechanical stress along the rim is likely to cause a sharp variation in the potential experienced by the vortex causing it to become pinned. Due to the reproducibility of the vortex creation for both orientations of the current, we ascribe this effect to the Oersted field generated by the DC current rather than the STT effect.

At lower currents, close to the point that the microwave signal disappears, it is expected that the V-AV dynamics will remain under or within the vicinity of the NC, Fig. 5 shows magnetic images acquired at current values of  $-1\text{mA}$  and  $-5\text{mA}$  from a SL-STO device with  $\sim 50\text{nm}$  NC diameter. The observed features may indicate magnetization dynamics in the region where the NC is positioned (red arrow in Fig. 5). Due to the time-averaged nature of the measurements it is not possible to determine a trajectory for the vortex. However, it is still possible to observe changes in the time-averaged magnetic contrast that occur at different current values. It is expected that at  $-1\text{ mA}$  the V-AV dynamics disappear due to the small

current density. At  $-5\text{mA}$  the magnetization dynamics underneath the contact generate a low frequency microwave signal and some change in the magnetization is expected to occur. The comparison between these two current values is made in Fig. 5 (b) and (c). While the appearance of two dark spots is suggestive of magnetic contrast associated with time-averaged vortex motion, it is impossible to completely rule out the breakthrough of structural features into the magnetic images. Further testing of the reconstruction process on model systems is required to confirm this latter interpretation.

#### IV. CONCLUSION

In conclusion, we have presented time-averaged images of the magnetization within single layer NC STO devices with 100 nm and 50 nm nano-contact diameter. Transport measurements showed a response characteristic of the vortex – antivortex dynamics that have been previously reported [10], making the devices good candidates for imaging by x-ray holography techniques. HERALDO measurements suggest pinning of a vortex at the rim of the aperture within the Au mask for a device with 100nm NC diameter at DC current values of  $-24\text{mA}$  and  $24\text{mA}$ . For smaller current values, devices with a 50nm NC diameter showed changes in the time averaged magnetic contrast that may indicate the presence of a dynamic process within vicinity of the NC. Since the x-ray beam has a well-defined time structure, time resolved stroboscopic measurements should be possible in future by injection locking to a multiple of the synchrotron master oscillator frequency.

#### ACKNOWLEDGMENT

The author was supported by CONICYT–Becas Chile. P. Keatley was supported by EPSRC grant EP/I038470/1.

#### REFERENCES

- [1] J. C. Slonczewski. “Current-driven excitation of magnetic multilayers”, *J. Magn. Magn. Mater.* 159:L1, 1996.
- [2] V.S. Pribyl, I.N. Krivorotov, G.D. Fuchs, P.M. Braganca, O. Ozatay, J.C. Sankey, D.C. Ralph, and R.A. Buhrman, “Magnetic vortex oscillator driven by d.c.spin-polarized current”, *Nat Phys.*, vol. 3, p. 498, 2007.
- [3] A. Dussaux, B. Georges, J. Grollier and V. Cros, A. V. Khvalkovskiy and A. Fukushima M. Konoto and H. Kubota, K. Yakushiji, S. Yuasa, K. A. Zvezdin, K. Ando and A. Fert, “Large microwave generation from current-driven magnetic vortex oscillators in magnetic tunnel junctions”. *Nature comms.*, Vol 1, 8, 2010.
- [4] E. B. Myers, D. C. Ralph, J. A. Katine, R. N. Louie and R. A. Buhrman., *Science* 285, 867, 1999.
- [5] Y. Ji, C. L. Chien, and M. D. Stiles, *Phys. Rev. Lett.* 90,106601, 2003.
- [6] B. Ozyilmaz, A. Kent, J. Sun, M. Rooks, and R. Koch, “Current-induced excitations in single cobalt ferromagnetic layer nanopillars”, *Phys. Rev. Lett.*, vol. 93, no. 17, p. 176604, 2004.
- [7] B. Ozyilmaz and A. D. Kent, “Current-induced switching in single ferromagnetic layer nanopillar junctions”, *Appl. Phys. Lett.*, vol. 88, no. 16, p. 162506, 2006.
- [8] Y. Pogoryelov, P. K. Muduli, S. Bonetti, E. Iacocca, F. Mancoff and J. Åkerman, “Frequency modulation of spin torque oscillator pairs”, *Appl. Phys. Lett.*, vol 98, p. 192501, 2011.
- [9] Y. Pogoryelov, P. K. Muduli, S. Bonetti, F. Mancoff and J. Åkerman, “Spin-torque oscillator linewidth narrowing under current modulation”, *Appl. Phys. Lett.*, vol 98, p. 192506, 2011.

- [10] M. Poliansky and P. Brouwer, “Current-induced transvers spin-wave instability in a thin nanomagnet”, *Phys. Rev. Lett.*, vol. 92, no. 2, p. 026602, 2004
- [11] M. Stiles, J. Xiao, and A. Zangwill, “Phenomenological theory of current-induced magnetization precession”, *Phys. Rev. B.* vol. 69, no. 5, p. 054408, 2004.
- [12] S. R. Sani, P. Drrenfeld, S. M. Mohseni, S. Chung, J. Akerman, “Microwave signal generation in Single-Layer Nano-Contact Spin Torque Oscillators”, *IEEE Trans. Magn.* Vol 49, no. 7, pp. 4331–4334, 2013.
- [13] S. Petit-Watelot, J.-V. Kim, A. Ruotolo, R. M. Otxoa, K. Bouzehouane, J. Grollier, A. Vansteenkiste, B. Van de Wiele, V. Cros and T. Devolder, “Commensurability and chaos in magnetic vortex oscillations”, *Nature Phys.* vol. 8, pp. 682–687, 2012.
- [14] D. V. Berkov and N. L. Gorn, “Spin-torque driven magnetization dynamics in a nanocontact setup for low external fields: Numerical simulation study”. *Phys. Rev. B* vol. 80, 064409, 2009.
- [15] T. A. Duckworth, F. Ogrin, S. S. Dhesi, S. Langridge, A. Whiteside, T. Moore, G. Beutier, and G. van der Laan, “Magnetic imaging by X-ray holography using extended references,” *Opt. Express.* 19, 16223–16228, 2011.
- [16] T. A. Duckworth, F. Y. Ogrin, G. Beutier, S. S. Dhesi, S. A. Cavill, S. Langridge, A. Whiteside, T. Moore, M. Dupraz, F. Yakhov, and G. v. d. Laan, “Holographic imaging of interlayer coupling in Co/Pt/NiFe,” *New J. Phys.* 15, 023045, 2013.